

# Broadband time-domain-reflectometry dielectric spectroscopy using variable-time-scale sampling

N. E. Hager III<sup>a)</sup>

Research and Development, Armstrong World Industries, Lancaster, Pennsylvania 17601

(Received 18 January 1993; accepted for publication 10 January 1994)

Methods for increasing the bandwidth of time-domain-reflectometry (TDR) dielectric spectroscopy using variable-time-scale sampling are presented. Consecutive segments of the TDR transient are sampled with increasing time increments and the entire transient transformed into the frequency domain using a running Laplace transform. Instrumentation artifacts are identified and controlled by examining reflected transients for stray artifacts prior to transformation, either on individual time scales or on a composite log time scale. Transform algorithms are verified using SPICE simulation in both time and frequency domains. Results are presented for a conducting salt solution, showing continuous dielectric spectra from 100 kHz to 5 GHz in the frequency domain, and requiring acquisition over six decades of time in the time domain to capture the entire response.

## I. INTRODUCTION

Time-domain-reflectometry (TDR) dielectric spectroscopy is an increasingly popular method for measuring broadband dielectric behavior at VHF and microwave frequencies.<sup>1,2</sup> In this and other work, the response of the material to a fast rising voltage step is measured in the time domain and converted to the frequency domain using a Laplace transform. Measurements are made along a coaxial transmission line with the sample mounted in a capacitive sample cell that terminates the line. An incident voltage step  $v(t)$  is applied to the line and recorded, along with the reflected voltage  $r(t)$  returned from the sample but delayed by the cable propagation time. For nonpolar dielectric samples (frequency-independent permittivity), the reflected signal follows the  $RC$  exponential response of the line-cell arrangement; for samples showing frequency dispersion, the signal follows the convolution of the instrument response with the charge transfer properties of the sample. With the introduction in the 1980s of highly stable TDR oscilloscopes with input bandwidths over 10 GHz and voltage step transition times around 35 ps, dielectric measurements in the multi-GHz range are now possible.

One factor limiting the bandwidth and resolution of the measurement is the use of constant sample intervals during acquisition. Equispaced sampling presents an experimental compromise between the resolution needed near the beginning of the detected signal and the total sampling time necessary to capture the entire response. If the sampling interval is chosen small to accentuate short time behavior the long time response is truncated; if the interval is chosen large to capture the entire response the short time resolution is degraded according to Shannon's sampling theorem.<sup>3</sup> An obvious solution is to use nonuniform sampling: sample the signal with short intervals near the beginning of the transient where the response changes rapidly and increase the sampling interval at later stages where the

response becomes more gradual. Such an approach has been used for some time at lower frequencies.<sup>4,5</sup> For the shortest exponential response (nonpolar materials), sampled with 12 bit vertical resolution, roughly two decades of variation between the initial and final sampling intervals could be expected without exceeding the limits of resolution at either extreme. For longer responses (dispersive materials) the expected variation in sampling interval would be even greater.

One approach to nonuniform sampling at high frequencies involves stepping the sampling interval logarithmically,<sup>6</sup> though to our knowledge there is no instrument commercially available with such capability. Another method, described in this work, involves sampling consecutive segments of the transient on increasing linear time scales and linking the entire response onto a composite time scale. This approach uses standard instrumentation, and has the advantage of allowing specific features in the wave form, such as leading edge behavior or multiple line reflections, to be analyzed on linear time scales. Frequency domain transformations are performed using a running Laplace transform over all time scales. As an example we present measurements for a conducting salt solution, showing strong effective dispersion in the frequency domain and requiring acquisition over six orders of magnitude in the time domain to capture the entire response.

## II. BACKGROUND

The basic relations governing transient response in the time domain and complex frequency behavior are described elsewhere by Cole,<sup>1</sup> Fellner-Feldegg,<sup>2</sup> and others. A voltage step, propagating along a line of characteristic admittance  $G$ , produces a voltage transition  $v(t)$  at the sample end. This combines with the reflected voltage  $r(t)$  to produce a combined voltage across the sample [ $v(t) + r(t)$ ]. Accompanying the voltage step is a current step  $Gv(t)$ , which combines with a reflected current  $-Gr(t)$  (sign indicating direction) to produce a combined sample current  $G[v(t) - r(t)]$ . The frequency components of sam-

<sup>a)</sup>Present address: Physics Dept., Franklin and Marshall College, Lancaster, PA 17604.

ple voltage and current are given by  $[v(\omega) + r(\omega)]$  and  $G[v(\omega) - r(\omega)]$ , respectively, where  $v(\omega)$  and  $r(\omega)$  are the complex Laplace transforms of  $v(t)$  and  $r(t)$ . Knowing the frequency components of sample voltage and current, the terminating sample admittance is then given as

$$Y(\omega) = G \frac{v(\omega) - r(\omega)}{v(\omega) + r(\omega)} \quad (1)$$

with the complex sample permittivity given as

$$\epsilon(\omega) = \frac{Y(\omega)}{i\omega C_0}, \quad (2)$$

where  $C_0$  is the geometric capacitance of the empty sample cell.

Differential methods are used to minimize connecting line distortions and establish a common time reference, since  $v(t)$  and  $r(t)$  are not measured directly at sample terminals but rather at the opposite end of the connecting line. The time delay between  $v(t)$  and  $r(t)$  creates an ambiguity in establishing a common zero time, making short time behavior suspect. Replacing the incident voltage with the empty cell reflection or other calibration reference reduces the errors in zero time to the limits of jitter and drift in the oscilloscope. The reflected sample signal  $r_x(t)$  is compared against the reflected signal  $r_r(t)$  from the calibrated reference instead of  $v(t)$ . The basic relation is found by writing the Eq. (1) for both reference and unknown, and solving to eliminate  $v(\omega)$ . The result is

$$\frac{Y_x(\omega)}{G} - \frac{Y_r(\omega)}{G} = \frac{\{1 - [Y_r(\omega)/G]^2\} \rho(\omega)}{1 + [Y_r(\omega)/G] \rho(\omega)} \quad (3)$$

with a reflection coefficient given by

$$\rho(\omega) = \frac{r_r(\omega) - r_x(\omega)}{r_r(\omega) + r_x(\omega)}, \quad (4)$$

where  $\epsilon(\omega) = Y(\omega)/i\omega C_0$  is then substituted for both reference and unknown admittances.

### III. ACQUISITION

Signals are both generated and detected by a HP 54120 digitizing oscilloscope equipped with the 54121A TDR sampling head. The scope has a 20 GHz input bandwidth with a 35 ps transition duration voltage step across one input. The cell loading is chosen such that the unknown signal is resolvable from both open- and short-circuit base lines, and thus the reference signal, over the time aperture required for Laplace transform ( $1/\omega_2 < t < 1/\omega_1$ , where  $\omega_1$  and  $\omega_2$  are the lower and upper frequency limits). In general, this amounts to adjusting either the sample area or thickness to achieve the necessary capacitance and decay time. In the present example, a HP 85070A dielectric surface probe, modified to a parallel-plate geometry, provides the sample cell. The 85070A is essentially a short 50  $\Omega$  transmission section which terminates in a flat measurement plane; a small parallel-plate cell is formed by attaching the reference ground clip, supplied with the probe, across the probe tip but separated from the tip by a thin metal spacer (Fig. 1). The spacer thickness is then ad-

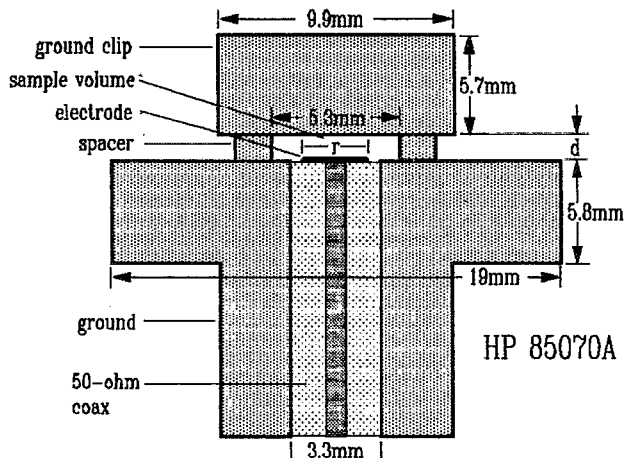


FIG. 1. Sample cell configuration, showing HP 85070A surface probe with spacer and attached ground clip. Spacer thickness ( $d$ ) and tip radius ( $r$ ) adjusted for loading.

justed to achieve the correct capacitance or, in the case of the Teflon reference, the tip area is increased by sandwiching a thin metal disk between the sample and the probe tip.

Differential measurements allow the use of standard reflectance signals for a reference instead of the incident voltage. For each sample, an associated reference standard is also measured; the spacer thickness is usually adjusted in real time to bring the sample and reference transients into alignment. Timing differences due to changing spacer thicknesses are corrected later in either time or frequency domains. Reference sources typically used are either a low-loss solid whose permittivity is nearly frequency independent or an empty cell air gap. The reference cell capacitance must be determined accurately since, as seen in Eq. (3), it couples frequency-dependent terms into the differential admittance equation (the unknown cell capacitance appears only as a scaling factor). Although the capacitance can be calculated from the geometry, it is generally more accurate to determine it electrically, by measuring  $RC$  time constant of the reflected signal.

Data acquisition is PC automated; both the operation of the scope and the collection of data are handled through the IEEE-488 interface. The acquisition program steps the scope through the various time scales, collects and averages data, and stores the information on disk. The initial time scale is set to record the leading edge of the reflected signal and is set on a very fast sampling rate to accurately record its timing and shape. Subsequent time scales are set to record consecutive segments of the reflected signal and are set on increasingly slower sampling rates as the signal change becomes more gradual. The final time scale is set to record any remaining signal contribution and is set on a very slow sampling rate as the signal approaches the open circuit baseline. In all cases, each time scale is delayed to start at the conclusion of the previous time scale. The entire sequence is scanned repetitively with the signal for each segment stored in a running sum; in this manner, any long-term drift occurring between segments is averaged out.

Before transforming to the frequency domain, reflected signals are examined for unwanted instrumentation artifacts in the time domain, where such artifacts can be identified on the basis of propagation delay. Signals can be examined either on individual time segments or on a composite log time scale. Sources of these artifacts include reflections from connectors and line imperfections, parasitic oscillations in the sample cell, or discontinuities at the segment boundaries resulting from drift between segments. Of particular concern are artifacts that vary during differential measurement, since such variations add large unwanted difference signals to the reflection coefficient  $\rho(\omega)$ . Identifying this behavior requires examining the difference in reflected signal between reference and unknown, since differences in Laplace coefficient are related to differences in transient response. Since the HP 54120 uses 12 bit vertical resolution in its vertical A/D, variations as small as three orders of magnitude below full scale are measurable.

#### IV. TRANSFORMS

Laplace transforms are calculated by direct numerical integration, as the usual software fast Fourier transform algorithms do not handle the ranges of time and frequency described in this work. For each frequency, a numerical integration is performed over all time scales, with the integration interval  $dt$  adjusted for each time scale. The contribution for a particular segment is calculated according to

$$v_n(\omega) = \int_{t_{ni}}^{t_{nf}} v(t) e^{-i\omega t} dt, \quad (5)$$

where  $t$  denotes the time relative to the reflection start,  $v(t)$  is the voltage relative to the open circuit baseline, and  $t_{ni}$  and  $t_{nf}$  are the start and stop times for segment  $n$ . The contributions for all segments are added together, along with a series of patch terms which correct slight timing mismatches at the segment boundaries. The patch terms are calculated by evaluating the integral contribution, using a simple trapezoidal rule, between the last data point on one time segment and the first data point on the next. At the stop time, the integration is either truncated at an integer number of cycles or extrapolated to infinity with the final contribution calculated analytically. The calcula-

tion is repeated for each frequency being analyzed, and the results stored as an array of logarithmically spaced Laplace coefficients. As a check of accuracy, the measured transient is replaced by a simulated transient whose transform is well known (e.g.,  $e^{-t/\tau}$ ); the calculated results are then compared with the expected ones.

Computational problems develop on longer time scales where the rate of sinusoidal variation exceeds the data point spacing. The following method of integration is thus used: (a) the trace is divided into a series of either two- or three-point intervals; (b) an analytic function is fit to each interval, a straight line in the case of two-point intervals or parabola in the case of three-point intervals; (c) the function is integrated analytically along with the sinusoidal variation over each interval; (d) the contribution for all intervals are added together numerically. This approach is insensitive to the rate of sinusoidal variation and can be used over all frequencies and time scales. The method basically amounts to a modified Simpson's or Trapezoidal integration rule, in which the sinusoidal variation is implicitly built in. In most cases, the three-point method produces less computational divergence.

Complex permittivity values are obtained by substituting Laplace coefficients for both reference and unknown in Eqs. (3) and (4). Adjustments are first made, however, to correct the vertical offset and remove any horizontal timing errors between arrays. The vertical adjustment is necessary since the coefficients in Eq. (5) are calculated relative to the open circuit base line while  $r_r(\omega)$  and  $r_x(\omega)$  are calculated relative to the baseline preceding the reflection. The correction is made, in the frequency domain, by adding a term  $(\Delta V/\omega)i$  to each element, where  $\Delta V$  is the vertical shift between baselines. Timing errors become a problem if the horizontal position of the pulse drifts between measurements; this is determined by noting the position of the leading edge of the reflection on the fastest time scale. This error is similarly removed, in the frequency domain, by multiplying one array by the term  $e^{-i\omega\Delta t}$ , where  $\Delta t$  is the time shift between traces.

Various checks and simulations ensure accuracy. As a check of instrument stability, two reference transients, taken under identical circumstances but at different times, are compared differentially. Treating one as the unknown, its permittivity is calculated and compared with the ex-

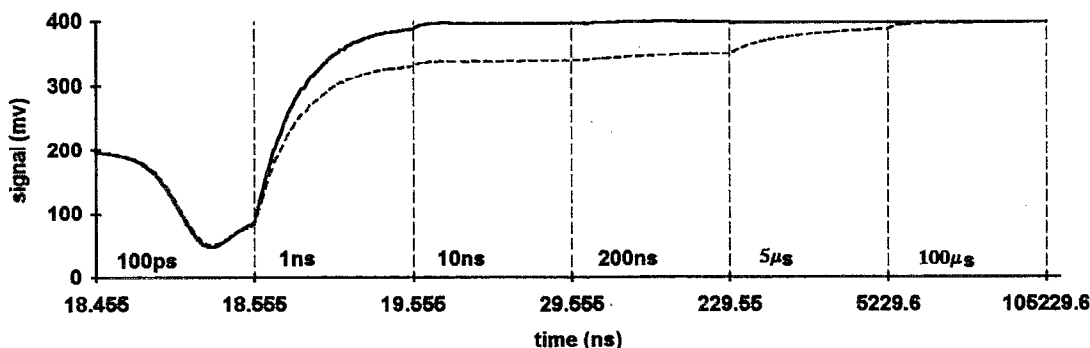


FIG. 2. Reflected signal from 0.03 M KCl solution (dashed) and Teflon reference standard (solid), sampled over six time scales.

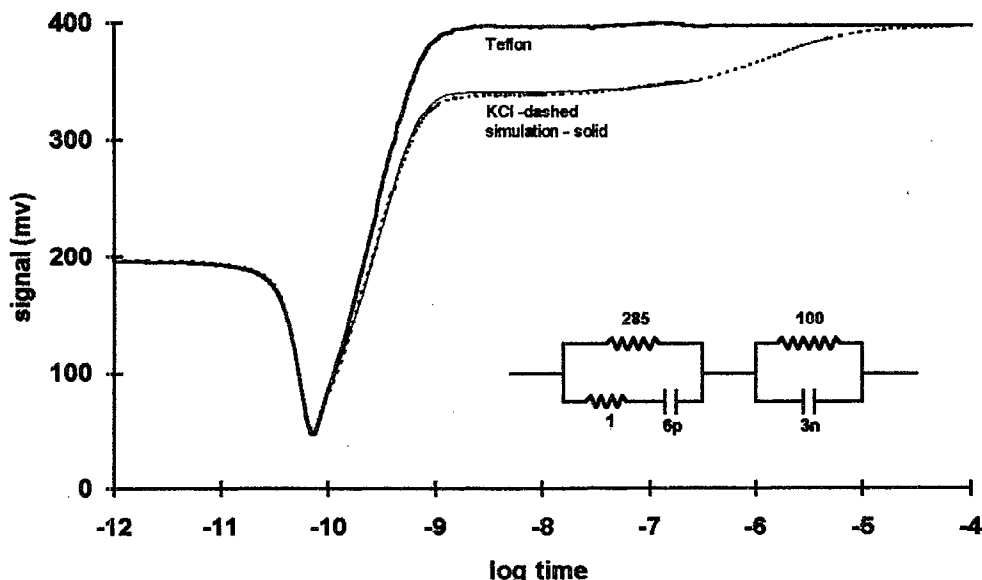


FIG. 3. Figure 2 data on combined log time scale. Upper trace is Teflon (solid), lower trace is KCl (dashed). Response of simulated model (inset) overlays KCl signal.

pected  $\epsilon^*(\omega) = 1$ ; any roll-off or "negative permittivity" indicates a problem with instrument drift. Another check involves using an electrical simulation program, such as SPICE,<sup>7</sup> to create an approximate electrical model for the material and simulate its response in both time and frequency domains. The resulting simulation is then compared with actual results in both domains.

## V. RESULTS

Figure 2 shows the reflected signals for a 0.03 M solution KCl in water and a Teflon reference standard, both sampled over six time scales. The KCl adds an ionic conductivity to the water, resulting in a strong effective dispersion due to electrode polarization. For both signals, acquisition begins at a point following the applied voltage step but preceding any significant rise in reflected signal (the actual starting time is arbitrary, since a common time shift cancels). The initial trace is recorded at a speed of 100

ps/scale, or 0.25 ps/digitized channel, so as to accurately record the position and shape of the leading edge. A 1 ps drift between reference and unknown is noted on this scale, and corrected later in the frequency domain. Succeeding segments are recorded at speeds of 1, 10, 200 ns, 5  $\mu$ s, and 100  $\mu$ s/full scale, continuing until the signal has completely decayed to the open circuit baseline. Dispersion in the KCl is obvious, even in the raw time data, as the signal decays only slowly to the open circuit base line even on longer time scales. The Teflon reference signal, on the other hand, decays rapidly to the open circuit baseline and follows an exponential RC law with a cell capacitance of 5.42 pf at the vertical midpoint.

Figure 3 shows the same data linked together onto a common log time scale; the combined signal splices smoothly at the segment boundaries and shows a clear resolvable signal from around  $10^{-10}$  to  $10^{-5}$  s. Overlaid on the data is a SPICE simulation of an approximate electrical model of the sample: a bulk conduction element including

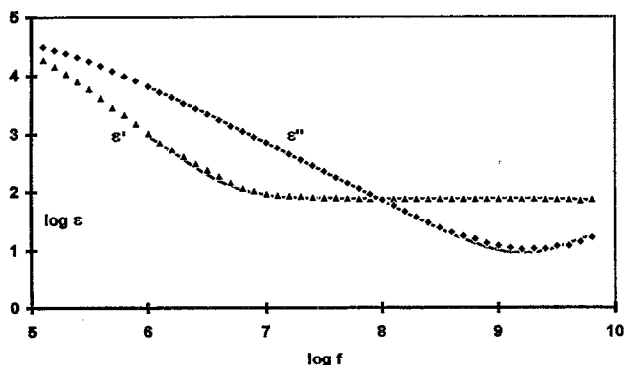


FIG. 4. Figure 2 data transformed to frequency domain, including simulation overlay. Large low-frequency values for relative permittivity  $\epsilon'$  and  $\epsilon''$  result from conductivity and electrode polarization.

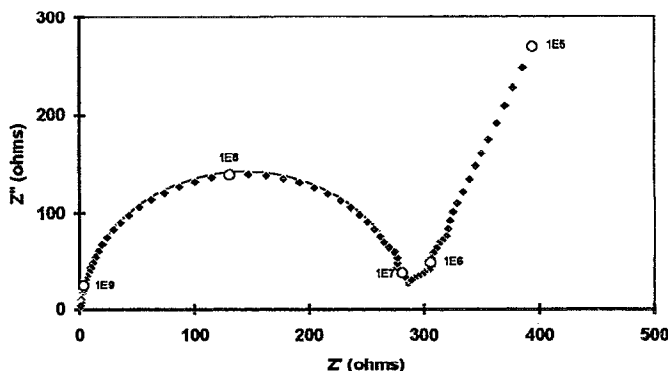


FIG. 5. Figure 2 data in complex impedance plane, including simulation overlay. Labeled parameter is frequency.

a high frequency rotator and an interfacial barrier element. Although the model certainly oversimplifies the physical situation, it does provide an independent check of the transform algorithm since the same circuit can now be simulated in both time and frequency domains. It also provides a simple means of predicting the transient response given the expected frequency behavior, and thus of determining whether the predicted response is within the resolution of the measurement.

Figures 4 and 5 show the permittivity and impedance data, respectively, transformed to the frequency domain along with the corresponding SPICE simulation. Figure 4 shows the real and imaginary parts of the complex permittivity plotted against frequency on a log frequency scale; Fig. 5 shows the real and imaginary parts of the complex impedance plotted against one another on a complex impedance plane. The large increases in  $\epsilon'$  and  $\epsilon''$  at low frequencies are the result of bulk conductivity and electrode polarization, as evidenced by the semicircular arc appearing in the corresponding impedance plane. The conductivity falls off above 1 GHz, as the permittivity approaches values expected for pure water.

## VI. DISCUSSION

We have demonstrated methods for performing broadband TDR dielectric spectroscopy at VHF/microwave frequencies using variable time scale sampling. In the example shown, frequency measurements of more than four orders

of magnitude are possible because strong dispersion in the sample material maintains a measurable cell impedance over a wide range. In less dispersive materials the bandwidth is reduced, though measurements of at least two orders of magnitude are still possible with considerable precision at the endpoints. Fewer time scales are required, but a tighter control of reflections from the lines and connectors is necessary as reference and unknown signals become nearly identical. Finally, measurements should not be limited to the particular electrode geometry discussed; it should be possible to extend these techniques to a variety of electrode sizes and geometries for different frequency ranges, sample thicknesses, and permittivities.

## ACKNOWLEDGMENTS

The author would like to acknowledge the many helpful discussions with Dr. J. G. Berberian of St. Joseph's University, Dr. A. J. Yang of Armstrong, and the late Professor R. H. Cole of Brown University.

<sup>1</sup>R. H. Cole, J. G. Berberian, S. Mashimo, G. Chryssikos, A. Burns, and E. Tombari, *J. Appl. Phys.* **66**, 793 (1989).

<sup>2</sup>H. Fellner-Feldegg, *J. Phys. Chem.* **73**, 616 (1969).

<sup>3</sup>C. Shannon, *Proc. IRE* **37**, 10 (1949).

<sup>4</sup>F. I. Mopsik, *Rev. Sci. Instrum.* **55**, 79 (1985).

<sup>5</sup>P. J. Hyde, *Proc. IEE* **117**, 1891 (1970).

<sup>6</sup>I. V. Ermolina, E. A. Polygalov, G. D. Romanychev, Yu. F. Zuev, and Yu. D. Feldman, *Rev. Sci. Instrum.* **62**, 2262 (1991).

<sup>7</sup>P-SPICE, Evaluation Version 5.1 for Windows, MicroSim Corporation, 20 Fairbanks, Irvine, CA 92718.